Temporal Quantum Fluctuations in Stimulated Raman Scattering: Coherent-Modes Description

M. G. Raymer

Department of Physics and Chemical Physics Institute, University of Oregon, Eugene, Oregon 97403

Z. W. Li

Laboratory for Laser Energetics, University of Rochester, Rochester, New York 14627

I. A. Walmsley

Institute of Optics, University of Rochester, Rochester, New York 14627

Temporal quantum fluctuations of the intensity of light pulses produced in the linear regime of stimulated Raman scattering are observed. A theoretical description based on the concept of coherent temporal modes is presented. The method makes use of a minimum number of random variables, which are the excitation amplitudes of the temporal modes, and allows an estimate of the probability for generating a Stokes pulse that is likely to form a soliton in the nonlinear propagation regime.

Several interesting aspects of the generation of macroscopic light fields by quantum-initiated stimulated Raman scattering (SRS) have been clarified in recent years. Using the Heisenberg-picture quantum theory of SRS,[1,2] full-scale fluctuations of macroscopic Stokes-pulse energies were predicted[3] and observed.[4,5] The agreement between theory and experiments supports the assertion that the statistics of the spontaneously generated Stokes field are thermal-like (i.e., Gaussian) in the absence of molecular saturation or pump-laser depletion. In parallel developments, Drühl, Wenzel, and Carlsten reported the first observations of soliton pulses in SRS when the pump laser pulse was strongly depleted.[6,7] It was determined that the soliton pulses were associated with a π phase shift in the Stokes field. It was pointed out by Englund and Bowden that these spontaneous solitons could arise naturally from the quantum-noise-driven phase fluctuations expected to occur during the buildup process of the Stokes pulse.[8] A connection was made also to the so-called phase waves predicted earlier by Hopf to occur in two-level superfluorescence.[9] Thus, the Stokes pulse-energy fluctuations and the spontaneous soliton formation are thought to arise from the same underlying mechanism: quantum-noise–driven temporal fluctuations of the Stokes field as it builds up from the zero-point motion of the molecular oscillators (or, equivalently, vacuum fluctuations of the radiation field).

This paper presents direct observations of the temporal quantum fluctuations of the Stokes pulse intensities, and offers a powerful and intuitive method for their analysis and interpretation. By decomposing the Stokes field into "coherent temporal modes," the nature of the fluctuations is described in terms of a minimum number of random variables. The fluctuations of the SRS frequency spectrum resulting from exciting more than one temporal mode were first reported by MacPherson, Swanson, and Carlsten.[10]

The observations were made using a Q-switched Nd-doped yttrium aluminum garnet laser, with frequency-doubled output pulses with wavelength 532 nm, duration $\tau_L = 7$ nsec (FWHM), and energy 2 mJ. The laser was injection seeded to ensure single-longitudinal-mode operation. The laser beam was collimated to a cross-sectional area (intensity half maximum) of $A = 2.8 \times 10^{-3}$ cm^2 and passed through a cell of length $L = 50$ cm containing H$_2$ at 100 atm, with a $Q(1)$ collisional linewidth (HWHM) of $\Gamma = 1.7 \times 10^{10}$ rad/sec (Ref. 11). The resulting Fresnel number $A/\lambda L$ of the interaction region was equal to 0.8, leading to a near-diffraction-limited generated Stokes beam at 680 nm. The gain coefficient is estimated to be $g = 0.33$ cm^{-1} for these conditions,[11] leading to an observed average energy conversion efficiency of 3%. The coherence time of the generated Stokes light is estimated to be $2(gL)^{1/2}\Gamma \simeq 0.7$ nsec.[2] Since the generated pulses have duration of about 2 nsec, some phase amplitude modulation is to be expected. The Stokes pulse intensities were recorded with a streak camera having a resolution of 30 psec.

Figure 1 shows eight examples of typical Stokes pulses observed under these conditions (out of an ensemble of about 100 pulses). The differences in shapes and integrated energies are believed to be due solely to quantum uncertainties in the initiation process. Of the many temporal shapes recorded, the symmetric shapes (a), (b), and (e) were observed occasionally. The random occurrence of these simple, smooth shapes from a noise generator can be understood using the method of coherent temporal modes.

Since the Fresnel number $A/L\lambda$ is less than unity, the generated Stokes field is approximately spatially coherent.[12] Then the slowly varying Stokes-field operator $\hat{E}_s^{(-)}(t)$ at the output face $(z = L)$ of the generator cell is approximately independent of the transverse spatial coordinates and can be expanded in terms of a com-
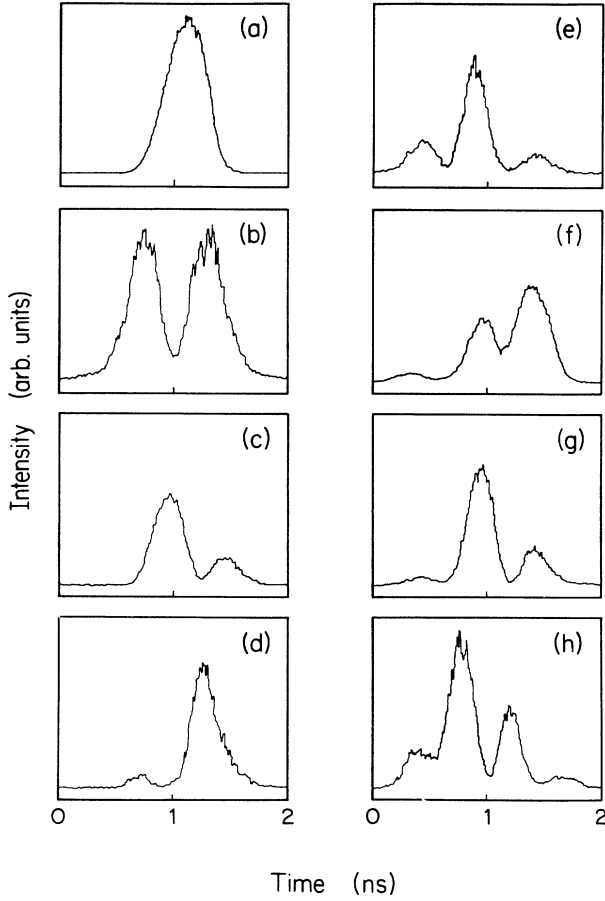
FIG. 1. Examples of random time evolution of Stokes pulse intensity, all occurring under identical conditions. The shapes are ordered roughly from most probable (a) to least probable (h). At lower H_2 gas pressure only single-peak shapes such as (a) are observed. The fast structure is noise in the streak camera.

plete, orthonormal set of temporal functions, $\Psi_i(t)$,

$$\hat{E}_s^{(-)}(t) = \left[\frac{2\pi\hbar\omega}{Ac}\right]^{1/2} \sum_{i=1}^{\infty} \hat{a}_i^\dagger \Psi_i(t), \qquad (1)$$

where ω is the Stokes frequency and $\hat{a}_i^\dagger$ is the photon creation operator for the "temporal mode" $\Psi_i(t)$.[12,13] The functions $\Psi_i(t)$ are taken to be orthonormal over a time period $[-T, T]$, where T is large enough that outside of this range the field amplitude is essentially zero. A useful choice of the mode functions is found by requiring that the modes be statistically uncorrelated, i.e.,

$$\langle \hat{a}_i^\dagger \hat{a}_j \rangle = \bar{n}_i \delta_{ij}, \qquad (2)$$

where $\bar{n}_i$ is the quantum expectation value (ensemble average) of the number of photons in mode $\Psi_i(t)$. That this condition uniquely determines the mode functions can be seen by calculating the two-time correlation func-
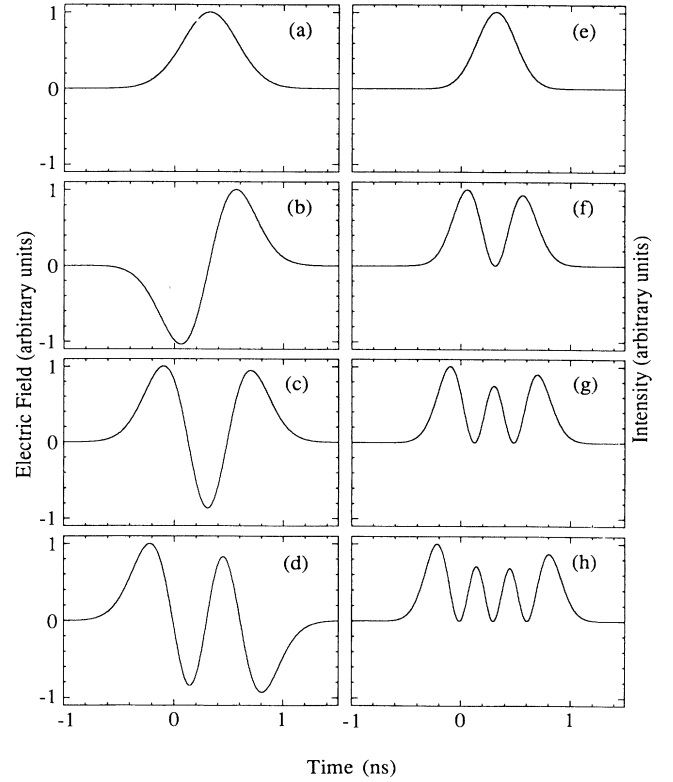

FIG. 2. (a)–(d) Four lowest-order temporally coherent modes, $\Psi_1(t)$–$\Psi_4(t)$, calculated as eigenfunctions of Eq. (4) for the same conditions as the data in Fig. 1. Curves (e)–(h) are the squares of the same four mode functions. The Gaussian-shaped pump pulse, with duration (FWHM) 7 nsec, is centered at $t = 0$.

tion of the field (at $z = L$),

$$G(t_1, t_2) = \frac{Ac}{2\pi\hbar\omega} \langle \hat{E}_s^{(-)}(t_1)\hat{E}_s^{(+)}(t_2) \rangle$$

$$= \sum_i \bar{n}_i \Psi_i(t_1)\Psi_i^*(t_2), \qquad (3)$$

where Eqs. (1) and (2) were used. Equation (3) can easily be inverted, using the mode orthonormality to find

$$\int_{-T}^{T} G(t_1, t_2)\Psi_j(t_2)dt_2 = \bar{n}_j\Psi_j(t_1). \qquad (4)$$

Equation (4) is an integral eigenvalue problem, and $G(t_1, t_2)$ is a Hilbert-Schmidt kernel; therefore the eigenvalues $\bar{n}_j$ are real and the eigenfunctions $\Psi_i(t)$ are complete. The mode expansion (1) is called a Karhunen-Loeve expansion, and is similar to that used in classical coherence theory.[14] It is important to realize that the mode functions are independent of T, since we are dealing with a pulsed excitation. This is in contrast to the usual applications of the Karhunen-Loeve expansion, where the mode functions depend on the size of the interval used to define them.

The correlation function $G(t_1, t_2)$ is evaluated explicit-

ly from the one-dimensional quantum theory of SRS in the linear-gain regime.[12] Then Eq. (4) is solved numerically by converting the integral to a discrete sum over 80 points and using standard matrix-diagonalization techniques. This number of points is sufficient to ensure convergence in the sense that $\bar{n}_{80} \cong 0$. The four eigenfunctions with the largest eigenvalues $\bar{n}_j$ are shown in Figs. 2(a)–2(d). The squares (intensities) of the eigenfunctions are shown in Figs. 2(e)–2(h). The four largest eigenvalues are $\bar{n}_1 = 4.71 \times 10^{12}$, $\bar{n}_2 = 1.51 \times 10^{12}$, $\bar{n}_3 = 5.15 \times 10^{11}$, and $\bar{n}_4 = -1.85 \times 10^{11}$.

In order to determine the statistics of exciting various temporal modes, note that the Stokes field has Gaussian statistics,[3] and so each $\hat{a}_i^\dagger$ is Gaussian, with zero mean and variance $\bar{n}_i$. This fact, along with the uncorrelated property, Eq. (2), means that the $\hat{a}_i^\dagger$ are statistically independent. Thus the joint probability density for observing values of the (complex) mode amplitudes $a_1, a_2, a_3, \ldots$ is

$$P(a_1, a_2, a_3, \ldots) = \prod_{j=1}^{J} (\pi \bar{n}_j)^{-1} \exp(-|a_j|^2/\bar{n}_j), \quad (5)$$

where $J = 80$ is the number of mode functions found in the numerical solution of Eq. (4). Individual classical realizations of Stokes pulses can be constructed by summing Eq. (1) with random coefficients a_j^* determined numerically in accordance with Eq. (5). Several examples are shown in Figs. 3(a)–3(h). These are chosen from an ensemble that is of similar size ($\sim$100) to the experimental ensemble. The realizations are arranged in the figure to best show their similarity with the corresponding observed pulses in Fig. 1. The percentage of pulses having one, two, three, or four peaks is roughly consistent between the experimental and theoretical ensembles.

It is of interest to determine the probability $P_i(f)$ for a given mode $\Psi_i(t)$ to have at least a fraction f of the total pulse energy on a given shot. This is obtained by integrating Eq. (5) over the domain in which $|a_i|^2 \geq f \sum_j |a_j|^2$ to give

$$P_i(f) = \sum_{j \neq i}^{J} \frac{\bar{n}_j^{J-3}[1/\bar{n}_j + 1/(1-f)\bar{n}_i]^{-1}}{\prod_{k \neq i,j} (\bar{n}_j - \bar{n}_k)}. \quad (6)$$

For example, we estimate the probability for mode $\Psi_2(t)$ to contain at least 75% of the pulse energy to be $P_2(0.75) = 0.017$. This is in qualitative agreement with the observation that of 96 pulses observed, two looked similar to Fig. 2(b). By comparison, the probability for mode $\Psi_1(t)$ to contain at least 75% of the energy is predicted to be $P_1(0.75) = 0.24$, which is consistent with the experimental observation of 21 out of 96 pulses looking similar to that in Fig. 1(a). On the other hand, when the H_2 pressure is lowered to 50 atm, decreasing the Raman linewidth Γ by a factor of 2, virtually all of the Stokes pulses have a single peak, indicating that only the lowest-order temporal mode is excited in this case. This,
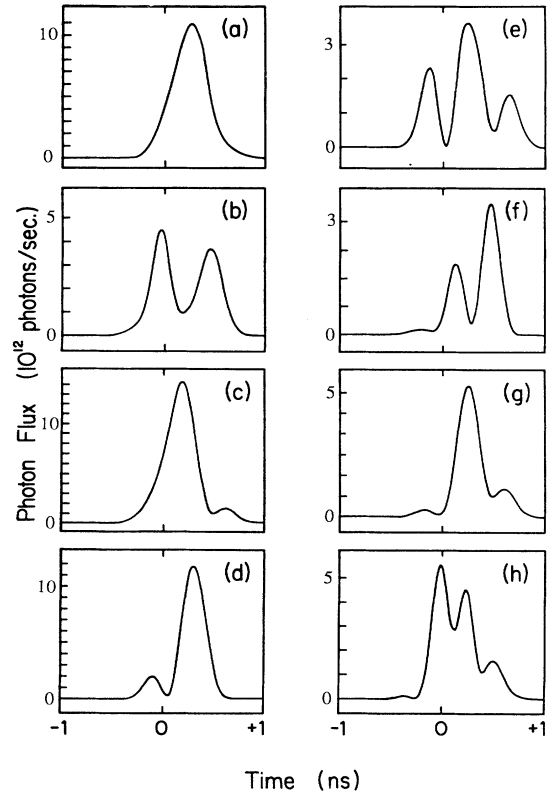

FIG. 3. Individual realizations of Stokes pulses obtained by adding up temporal mode functions [four of which are shown in Figs. 2(a)–2(d)], with random coefficients a_i, having probability density given by Eq. (5). The realizations are arranged to emphasize the similarity to the data in Fig. 1.

too, is consistent with our calculations.

It is important to note that mode $\Psi_2(t)$ [Fig. 2(b)] has exactly the correct π phase shift needed to induce the formation of a Raman soliton in free-space propagation.[6,7] Thus, a rough estimate of the probability to form spontaneously such a soliton is given by $P_2(f)$ from Eq. (6) with f chosen as, say, 0.9. For the conditions of the experiments of MacPherson, Swanson, and Carlsten ($\tau_L = 20$ nsec, $\Gamma = 1.7 \times 10^9$ rad/sec) with gL chosen as 30 to represent the scattering just before going into the saturated regime, we find a value $P_2(0.9) = 0.0037$. This is not inconsistent with the experimental observation of roughly five strong spontaneous solitons (with greater than 50% reversal of pump depletion) in every 1000 shots.[7]

In conclusion, the present work shows the existence of the temporal quantum fluctuations in the initiation regime of SRS and gives an intuitively appealing manner in which to view the formation of certain simple pulse shapes, including that shape with π phase shift. This phase shift is that which is required to form spontaneously the Raman soliton, as well as the phase wave in

superfluorescence.[9] It is intriguing that such a simple, smooth pulse as that in Fig. 2(b) can arise from the linear amplification of white quantum noise associated with spontaneous Raman scattering. The smoothing of initial noise is also evident in superfluorescence[15,16] and amplified spontaneous emission.[17]

The advantage of the coherent-temporal-modes description over the numerical simulation approach commonly taken[8,9,16] is in the greatly reduced number of random variables involved in the former. In the simulation approach the number of random variables required is equal to the number of space-time points (perhaps 10000) used for integration of the equations of motion. In the coherent-modes approach the number of random variables required is equal to the number of significantly excited modes (perhaps four or five when $\tau_L \sim 1/\Gamma$). While the coherent-modes approach is valid only in the linear (undepleted-pump) regime, significant insight into nonlinear evolution can still be obtained by considering the field generated in the linear regime to be the input for the nonlinear regime of amplification.[10]

[1]T. von Foerster and R. J. Glauber, Phys. Rev. A **3**, 1484 (1971).

[2]M. G. Raymer and J. Mostowski, Phys. Rev. A **24**, 1980 (1981).

[3]M. G. Raymer, K. Rzazewski, and J. Mostowski, Opt. Lett. **7**, 71 (1982).

[4]I. A. Walmsley and M. G. Raymer, Phys. Rev. Lett. **50**, 962 (1983).

[5]N. Fabricius, K. Nattermann, and D. von der Linde, Phys. Rev. Lett. **52**, 113 (1984).

[6]K. Drühl, R. G. Wenzel, and J. L. Carlsten, Phys. Rev. Lett. **51**, 1171 (1983).

[7]D. C. MacPherson, R. C. Swanson, and J. L. Carlsten, in *Optical Society of America 1988 Annual Meeting,* Technical Digest Series Vol. 11 (Optical Society of America, Washington, DC, 1988).

[8]J. C. Englund and C. M. Bowden, Phys. Rev. Lett. **57**, 2261 (1986).

[9]F. A. Hopf, Phys. Rev. A **20**, 2064 (1979).

[10]D. C. MacPherson, R. C. Swanson, and J. L. Carlsten, Phys. Rev. Lett. **61**, 66 (1988); Phys. Rev. A **39**, 3487 (1989).

[11]W. K. Bischel and M. J. Dyer, Phys. Rev. A **33**, 3113 (1986).

[12]M. G. Raymer, I. A. Walmsley, J. Mostowski, and B. Sobolewska, Phys. Rev. A **32**, 332 (1985).

[13]That $\hat{a}_i^\dagger$ is a boson operator can be seen by using orthogonality of the $\Psi_i(t)$ to invert Eq. (1) for $\hat{a}_i^\dagger$ in terms of $\hat{E}_s^{(-)}(t)$ and using the approximate one-dimensional commutation relation

$$[\hat{E}_s^{(-)}(z,t),\hat{E}_s^{(+)}(z',t')] = \frac{2\pi\hbar\omega}{Ac}\delta\left(t - \frac{z}{c} - t' + \frac{z'}{c}\right)$$

to prove that $[\hat{a}_i,\hat{a}_j^\dagger] = \delta_{ij}$.

[14]For example, B. Saleh, *Photoelectron Statistics. With Applications to Spectroscopy and Optical Communication,* Springer Series in Optical Sciences Vol. 6 (Springer-Verlag, New York, 1978), Sec. 4.1.3.

[15]H. M. Gibbs, Q. H. F. Vrehen, and H. M. Hikspoors, Phys. Rev. Lett. **39**, 547 (1977).

[16]F. Haake, H. King, G. Schroder, J. Haus, and R. Glauber, Phys. Rev. A **20**, 2047 (1979).

[17]M. S. Malcuit, J. J. Maki, D. J. Simkin, and R. W. Boyd, Phys. Rev. Lett. **59**, 1189 (1987).